A NEW FICTITIOUS DOMAIN METHOD IN SHAPE OPTIMIZATION

KARSTEN EPPLER, HELMUT HARBRECHT, AND MARIO MOMMER

ABSTRACT. The present paper is concerned with investigating the capability of
the smoothness preserving fictitious domain method from [22] to shape optimiza-
tion problems. We consider the problem of maximizing the Dirichlet energy func-
tional in the class of all simply connected domains with fixed volume, where the
state equation involves an elliptic second order differential operator with non-
constant coefficients. Numerical experiments in two dimensions validate that we
arrive at a fast and robust algorithm for the solution of the considered class of
problems. The proposed method keeps applicable for three dimensional shape op-
timization problems.

INTRODUCTION

In several papers (see [8, 9] for example), two of the authors developed efficient algo-
rithms for the solution of several elliptic shape optimization problems. A boundary
variational approach was proposed in combination with boundary integral represen-
tations of the shape gradient and the shape Hessian. The considered class of model
problems allowed the use of boundary integral equations to compute all ingredients
of the functional, the gradient, and the Hessian, that arise from the state equation.
In combination with a fast wavelet Galerkin method to solve the boundary integral
equations, we obtained very efficient first and second order algorithms for shape
problems in two and three spatial dimensions. In particular, the use of boundary
element methods requires only a discretization of the free boundary. In our opinion
this is very advantageous since, on the one hand, modern boundary integral methods
reduce the complexity, and on the other hand, large deformations of the domains are
realizable without remeshing. Moreover, exterior boundary value problems are treat-
able, like in the computation of free surfaces of liquid bubbles or drops levitating in
an electromagnetic field, cf. [10, 11].

However, to be able to realize the optimal efficiency from these advantages, it is
of great help if the constraints and shape derivatives can be formulated in terms
of *boundary integrals*. Consequently, further assertions on the objective have to be
made for the powerful application of boundary element methods, see [8] for the
details.

In case of compactly supported cost functionals one can overcome this restriction by coupling finite and boundary elements (see [12]). Thus, the advantages of both methods are retained, namely fast access to values on the compact subset by finite elements on a fixed triangulation and the simple treatment of the free boundary by boundary elements. Nevertheless, the restriction to state equations involving differential operators with *constant* coefficients remains.

However, the above mentioned techniques are not applicable to state equations involving elliptic differential operators with *non-constant* coefficients. Fictitious domain methods offer obviously a convenient tool to deal with such shape optimization problems while the complicated remeshing, required for finite element methods, is still avoided, see Haslinger et al. [15, 16], Kunisch/Peichl [21], Neitaanmäki/Tiba [25], and Slawig [29, 30].

Up to now, the success of fictitious domain methods was limited since traditional methods suffer from low orders of convergence. For instance, the fictitious domain-Lagrange multiplier approach converges only as $\mathcal{O}(h^{1/2})$ in the energy norm when approximating from uniform grids with mesh size h (see [18]). Even the rate of convergence of standard (i.e. based on isotropic refinements) adaptive methods is limited by $\mathcal{O}(N^{-1/2})$ and $\mathcal{O}(N^{-1/4})$ in two and three dimensions, respectively, when spending N degrees of freedom, independently of the order of the approximation spaces (see [23] for a more detailed discussion).

These difficulties arise from non-smooth extensions of the solutions outside the intrinsic domain. In [22, 23], one of the authors proposed a rather novel and promising *smoothness preserving* fictitious domain method which realizes higher orders of convergence due to smooth extensions of the solution. The present paper is devoted to demonstrate the capability of this method when used in the context of shape optimization problems.

We consider the problem of maximizing the Dirichlet energy functional in the class of all connected domains of class C^2, where the state solves a standard elliptic boundary value problem of second order. To ensure uniqueness the sought domain is supposed to have a given volume. For sake of clearness in representation, we restrict ourselves to the two dimensional setting. However, we emphasize that the present algorithms can be straightforwardly extended to three spatial dimensions.

The paper is organized as follows. Section 1 is dedicated to shape optimization. We introduce our model problem of maximizing the Dirichlet energy functional under a volume constraint. After deriving the shape derivatives, we consider a standard augmented Lagrangian algorithm to treat the volume constraint. The minimization problems in the inner loop are solved by a nonlinear Ritz-Galerkin method for the

necessary condition. A vector valued boundary perturbation ansatz is employed in order to describe the boundary and its update. On the one hand, any domain of gender zero can be represented, on the other hand, the boundary representation is non-unique. Since therefore the surface mesh might degenerate, we add a regularization term to the objective. In Section 2 we present the numerical scheme to compute the state function. We introduce the smoothness preserving fictitious domain method and discuss the evaluation of domain integrals by numerical quadrature. In the last section (Section 3) we present numerical results to demonstrate the capability of our approach.

1. SHAPE OPTIMIZATION

1.1. **The model problem.** Let $\Omega \subset \mathbb{R}^2$ be a domain with boundary $\Gamma := \partial\Omega$. We consider the Dirichlet energy functional

$$(1.1) \qquad J(\Omega) = \int_\Omega \langle \mathbf{A}\nabla u, \nabla u \rangle d\mathbf{x} = \int_\Omega f u d\mathbf{x},$$

where the state function u solves the boundary value problem

$$(1.2) \qquad \begin{aligned} -\operatorname{div}(\mathbf{A}\nabla u) &= f && \text{in } \Omega, \\ u &= 0 && \text{on } \Gamma = \partial\Omega. \end{aligned}$$

Herein, we assume that the inhomogenity $f : \mathbb{D} \to \mathbb{R}$ and the symmetric and positive matrix $\mathbf{A}(\mathbf{x}) = [a_{ij}(\mathbf{x})]_{i,j=1}^2$ are sufficiently regular and defined in a sufficiently large *hold all* $\mathbb{D} \subset \mathbb{R}^2$.

The goal of the present paper is to maximize the the Dirichlet energy (1.1) over the class Υ of admissible domains. We assign Υ to be the set of all simply connected domains of the class C^2. To ensure uniqueness we shall impose an equality constraint on the volume of the domain

$$(1.3) \qquad V(\Omega) := \int_\Omega d\mathbf{x} \overset{!}{=} V_0.$$

Consequently, we arrive at the following problem:

$$(P) \qquad -J(\Omega) \to \min_{\Omega \in \Upsilon} \quad \text{subject to} \quad V(\Omega) = V_0.$$

1.2. **Shape calculus.** We briefly recall well known facts about the first order shape calculus, useful for the discussion of the necessary condition and the numerical algorithms. For a general overview on shape calculus, mainly based on the perturbation of identity (Murat and Simon) or the speed method (Sokolowski and Zolesio), we refer the reader for example to Murat and Simon [24, 28], Pironneau [27], Sokolowski and Zolesio [31], Delfour and Zolesio [4], and the references therein.

Let $\mathbf{n}$ denote the outer unit normal to the boundary Γ and consider a C^2-smooth boundary perturbation field $\mathbf{U} : \Gamma \to \mathbb{R}^2$. Then, the shape gradient to the functional (1.1) reads as

$$(1.4) \qquad \nabla J(\Omega)[\mathbf{U}] = \int_\Gamma \langle \mathbf{U}, \mathbf{n} \rangle \langle \mathbf{A} \nabla u, \nabla u \rangle d\sigma,$$

since the local shape derivative $du = du[\mathbf{U}]$ satisfies

$$\mathrm{div}(\mathbf{A} \nabla du) = 0 \qquad \text{in } \Omega,$$

$$du = -\langle \mathbf{U}, \mathbf{n} \rangle \frac{\partial u}{\partial \mathbf{n}} \quad \text{on } \Gamma.$$

The gradient of the volume reads as

$$(1.5) \qquad \nabla V(\Omega)[\mathbf{U}] = \int_\Gamma \langle \mathbf{U}, \mathbf{n} \rangle d\sigma.$$

1.3. **Relaxation of the constraints.** The minimization problem (P) implies to find the solution $(\Omega^\star, \lambda^\star) \in \Upsilon \times \mathbb{R}$ of the saddle point problem

$$(\Omega^\star, \lambda^\star) = \arg \inf_{\Omega \in \Upsilon} \sup_{\lambda \in \mathbb{R}} L_\alpha(\Omega, \lambda),$$

where $L_\alpha(\Omega, \lambda)$ denotes the augmented Lagrangian functional

$$(1.6) \qquad L_\alpha(\Omega, \lambda) = -J(\Omega) + \lambda\big(V(\Omega) - V_0\big) + \frac{\alpha}{2}\big(V(\Omega) - V_0\big)^2.$$

Of course, the choice $\alpha = 0$ yields the pure Lagrangian while $\lambda = 0$ and $\alpha \to \infty$ is known as standard quadratic penalty method. However, both choices have some drawbacks from the numerical point of view, cf. [5, 19], for example.

In order to avoid these difficulties, we choose $\alpha > 0$ and consider the following standard augmented Lagrangian algorithm:

- initialization: choose initial guesses $\lambda^{(0)}$ for $\lambda^\star$ and $\Omega^{(0)}$ for $\Omega^\star$,
- inner iteration: solve

$$(1.7) \qquad \Omega^{(n+1)} := \mathrm{argmin}\, L_\alpha(\Omega, \lambda^{(n)})$$

  with initial guess $\Omega^{(n)}$,
- outer iteration: update

$$\lambda^{(n+1)} := \lambda^{(n)} - \alpha\big(V(\Omega^{(n+1)}) - V_0\big).$$

It is well known that the this algorithm converges to $(\Omega^\star, \lambda^\star)$ provided that α is appropriately chosen [5, 19].

Notice that the necessary condition to (1.6) is equivalent to the identity

$$\langle \mathbf{A} \nabla u, \nabla u \rangle \equiv \lambda^\star \quad \text{on } \Gamma^\star.$$

1.4. **Ritz-Galerkin approximation of the shape problem.** The boundary of a domain $\Omega \in \Upsilon$ can be parameterized by a bijective positive oriented curve

$$(1.8) \qquad \boldsymbol{\gamma} : [0,1] \to \Gamma, \quad \boldsymbol{\gamma}(\phi) = \begin{bmatrix} \gamma_x(\phi) \\ \gamma_y(\phi) \end{bmatrix},$$

such that

$$\gamma_x, \gamma_y \in C_{\mathrm{per}}^2([0,1]) := \left\{ f \in C^2([0,1]) : f^{(i)}(0) = f^{(i)}(1), \ i = 0,1,2 \right\}.$$

Setting

$$(1.9) \qquad \begin{aligned} \varphi_{-N}^\Gamma &:= \sin(2\pi N\phi), \varphi_{1-N}^\Gamma := \sin\left(2\pi(N-1)\phi\right), \ldots, \varphi_{-1}^\Gamma := \sin(2\pi\phi), \\ \varphi_0^\Gamma &:= 1, \varphi_1^\Gamma := \cos(2\pi\phi), \ldots, \varphi_N^\Gamma := \cos(2\pi N\phi), \end{aligned}$$

we define the space

$$(1.10) \qquad V_N^\Gamma = \mathrm{span}\{\varphi_{-N}^\Gamma, \varphi_{1-N}^\Gamma, \ldots, \varphi_N^\Gamma\} \subset C_{\mathrm{per}}^2([0,1])$$

of all trigonometric polynomials of degree $\leq 2N$. To discretize the shape optimization problem we make the ansatz

$$(1.11) \qquad \boldsymbol{\gamma}_N = \sum_{k=-N}^N \begin{bmatrix} a_k \\ b_k \end{bmatrix} \varphi_k^\Gamma \in V_N^\Gamma \times V_N^\Gamma$$

with coefficient vectors $[a_k, b_k]^T \in \mathbb{R}^2$. Identifying the approximate domain Ω_N with this boundary curve, problem (1.7) becomes finite dimensional

$$\Omega_N^\star := \mathrm{argmin}\, L_\alpha(\Omega_N, \lambda^{(n)}).$$

This discrete problem leads to a nonlinear Ritz-Galerkin scheme for the necessary condition:

$$\text{seek } \boldsymbol{\gamma}_N^\star \in V_N^\Gamma \times V_N^\Gamma \text{ such that } \nabla L_\alpha(\Omega_N^\star, \lambda^\star)[\mathbf{v}_N] = 0 \text{ for all } \mathbf{v}_N \in V_N^\Gamma \times V_N^\Gamma.$$

For the numerical solution of this nonlinear variational equation we apply the quasi-Newton method updated by the inverse BFGS-rule without damping. A second order approximation is proposed for performing the line search update if a descent fails. For all the details we refer to [5, 13, 14, 19] and the references therein.

Remark 1.1. *In the three dimensional case one considers the unit sphere $\mathbb{S}^2$ as parameter space and the ansatz spaces V_N^Γ consisting of spherical harmonics of order $\leq N$. Then, $\gamma_N : \mathbb{S}^2 \to \Gamma$ is defined according to*

$$\boldsymbol{\gamma}_N = \sum_k \mathbf{a}_k \varphi_k^\Gamma \in V_N^\Gamma \times V_N^\Gamma \times V_N^\Gamma$$

with coefficients $\mathbf{a}_k \in \mathbb{R}^3$. This ansatz has been used in e.g. [20].

1.5. **Regularization.** The ansatz (1.11) does not impose any restriction to the topology of the domain except for its gender. However, even though both components of $\boldsymbol{\gamma}$ are elements of $C^2_{\text{per}}([0,1])$, we cannot guarantee that $\Omega \in C^2$. Furthermore, the parametric representation (1.8) of the domain Ω is not unique. In fact, if $\Xi : [0,1] \to [0,1]$ denotes any smooth 1-periodic bijective mapping, then the boundary curve $\boldsymbol{\gamma} \circ \Xi$ describes another parameterization of Ω.

To avoid degenerated boundary representations we shall include a regularization term. It is quite obvious that, for numerical computations, a "nice" parameterization distributes equidistant grid points of $[0,1]$ equidistantly on Γ. This means that the mesh functional

$$(1.12) \qquad M(\Omega) = \int_0^1 (\langle \boldsymbol{\gamma}', \boldsymbol{\gamma}' \rangle - |\Gamma|^2)^2 d\phi,$$

becomes small since it vanishes only if Ω is parameterized with respect to the arc length. This motivates to solve for small $\beta > 0$ the regularized shape problem

$$(P') \qquad J(\Omega) + \beta M(\Omega) \to \min_{\Omega \in \Upsilon} \quad \text{subject to} \quad V(\Omega) = V_0$$

instead of the original problem (P). We mention that the best numerical results are achieved when $\beta \to 0$ during the optimization procedure.

Remark 1.2. *The three dimensional analogue of the mesh functional* (1.12) *is*

$$M(\Omega) = \int_{\mathbb{S}^2} \left\| \begin{bmatrix} \langle \boldsymbol{\gamma}_x, \boldsymbol{\gamma}_x \rangle & \langle \boldsymbol{\gamma}_x, \boldsymbol{\gamma}_y \rangle \\ \langle \boldsymbol{\gamma}_y, \boldsymbol{\gamma}_x \rangle & \langle \boldsymbol{\gamma}_y, \boldsymbol{\gamma}_y \rangle \end{bmatrix} - \frac{|\Gamma|^2}{|\mathbb{S}|^2} \mathbf{I} \right\|_F^2 d\sigma,$$

where $\| \cdot \|_F$ denotes the Frobenius norm. The mesh functional is identical to zero iff the first fundamental tensor of differential geometry is on the whole parameter space identical to $|\Gamma|^2/|\mathbb{S}|^2$-times the identity matrix.

2. Numerical Method to compute the State

2.1. **The SPFD method.** To compute the state given by (1.2) we use a close variant of the smoothness preserving fictitious domain (SPFD) method, introduced in [22]. The SPFD method is a fairly new domain embedding technique that has yet to be fully understood from a theoretical point of view. It has, however, performed well in experimental settings before, and as will be seen in the numerical results, it can fulfill its promise in more applied settings.

To solve a boundary value problem with any fictitious domain method, one embeds the *intrinsic domain* into a larger *fictitious domain*, for example, a periodic cube $\mathbb{T} = (\mathbb{R} \setminus \mathbb{Z})^2$. The next step is to construct from the original problem some auxiliary

problem on the fictitious domain such that the solutions of this auxiliary and the original problem coincide on the intrinsic domain.

We assume that the right hand side f is in $L^2(\mathbb{T})$. For sake of simplicity we shall assume from now on that the *hold all* satisfies $\mathbb{D} = \mathbb{T}$. Then, since the boundary is C^2, the solution of the state equation will be in $H^2(\Omega)$. Consider for a moment the more general, non-homogeneous boundary condition $u = g$ on Γ, with $g \in H^{3/2}(\Gamma)$, and consider the least-squares functional on $H^2(\mathbb{T})$,

$$(2.1) \qquad \Phi(u^+) = \|C(Au^+ - f)\|^2_{L^2(\mathbb{T})} + \|Bu^+ - g\|^2_{H^{3/2}(\Gamma)},$$

where $A : H^2(\mathbb{T}) \to L^2(\mathbb{T})$ is the differential operator, $B : H^2(\mathbb{T}) \to H^{3/2}(\Gamma)$ is the trace operator, and $C : L^2(\mathbb{T}) \to L^2(\mathbb{T})$ is such that Cv is the extension by zero of the restriction to Ω of $v \in L^2(\mathbb{T})$.

It is reasonably easy to check that Φ has a minimum, which is not unique but can be chosen to depend continuously on the data $b := [f, g]^T \in \mathcal{H} := L^2(\mathbb{T}) \times H^{3/2}(\Gamma)$. Thus, the operator $M : H^2(\mathbb{T}) \to \mathcal{H}$ associated with Φ, given by the operator matrix

$$M = \begin{bmatrix} CA \\ B \end{bmatrix},$$

is bounded, and, while it has a large kernel, it still has a bounded pseudoinverse. Furthermore, every minimizer of Φ is an extension of the solution to the original problem (see [22]). Thus, to compute the state, we shall solve the least-squares problem

$$(2.2) \qquad \text{find } u^+ \in H^2(\mathbb{T}) \text{ such that } \|Mu^+ - b\|_{\mathcal{H}} \to \min,$$

and take $u = u^+_{|\Omega}$.

2.2. Discretization and solution of the discrete problems.
To approximate solutions of (2.2), we will use dyadic grids of mesh size $h_j := 2^{-j}$, with $j \geq 0$ an integer. We write

$$\mathbb{T} = \bigcup_{\mathbf{k}=(k_x,k_y)\in\mathbb{Z}_j} Q_{j\mathbf{k}},$$

where $\mathbb{Z}_j := (\mathbb{Z}/2^j\mathbb{Z})^2$, and $Q_{j\mathbf{k}} := 2^{-j}[k_x, k_x + 1) \times [k_y, k_y + 1)$.

When trying to discretize the operator M on the given mesh, one quickly realizes that the operator C can yield a potentially fatal problem for the numerical implementation, as it implies the computation of quadrature problems on nontrivial domains, a task that usually is expensive. To overcome this problem, we approximate C by the operator C_j, defined as follows. Given $v \in L^2(\mathbb{T})$, C_jv is defined as

the extension by zero of the restriction of v to Ω_j, where

$$\Omega_j := \bigcup_{\mathbf{k} \in \mathbb{Z}_j} \{Q_{j\mathbf{k}} : Q_{j\mathbf{k}} \cap \Omega \neq \emptyset\}.$$

In practice, this choice also enhances the stability of the method.

Notice that this approximation is not as crude as it looks. It has been shown in [22] that if $C(Au^+ - f) = 0$, and $Au^+ - f \in H^s(\mathbb{T})$ for $s > 0$ such that $s - 1/2$ is not an integer, then

$$\|C_j(Au^+ - f)\|_{L^2(\mathbb{T})} \lesssim h_j^s \|Au^+ - f\|_{H^s(\mathbb{T})}.$$

Since one can always find such an extension u^+ whenever $u \in H^{s+2}(\Omega)$, this proves that the minimum of the modified least-squares functional

(2.3) $$\Phi_j(u^+) = \|C_j(Au^+ - f)\|_{L^2(\mathbb{T})}^2 + \|Bu^+ - g\|_{H^{3/2}(\Gamma)}^2$$

converges rapidly towards the minimum of Φ.

Next, let us choose suitable approximation spaces. In $H^2(\mathbb{T})$ we will approximate from the spaces

$$V_j^{\mathbb{T}} = \mathrm{span}\{\varphi_{j,\mathbf{k}}^{\mathbb{T}} : \mathbf{k} \in \mathbb{Z}_j\}$$

of periodic cardinal B-splines $\varphi_{j,\mathbf{k}}^{\mathbb{T}}$ of order $m > 2$ on the given grid. These are C^{m-2}-functions that are multi-polynomials of degree $m - 1$ on each cube $Q_{j\mathbf{k}}$. In $L^2(\mathbb{T})$ we will approximate using the spaces

$$V_j^0 = \mathrm{span}\{\varphi_{j,\mathbf{k},\mathbf{l}}^0 : \mathbf{k} \in \mathbb{Z}_j, \mathbf{l} \in \mathcal{I}\},$$

where $\mathcal{I} := \{\mathbf{l} = (l_x, l_y) : 0 \leq l_x, l_y < n\}$, consisting of dicontinuous piecewise multi-polynomials of order n. The orthonormal basis functions $\varphi_{j,\mathbf{k},\mathbf{l}}^0$ are supported on $Q_{j\mathbf{k}}$, defined as tensor products of Legendre polynomials up to degree $n - 1$. Note that $C_j V_j^0 \subset V_j^0$ greatly simplifies the calculation of entries in the system matrix. Finally, to approximate in $H^{3/2}(\Gamma)$, we use (after identifying Γ with $[0,1]$ by means of the parameterization (1.11)) the space $V_j^\Gamma := V_N^\Gamma$, where V_N^Γ is as defined in (1.10) with $N = 2^j$.

Next, we should introduce the discrete system matrices and load vectors. We have to compute

$$[\mathbf{A}_j]_{(\mathbf{k},\mathbf{l}),\mathbf{k}'} = -\int_{\Omega_j} \mathrm{div}(A\nabla\varphi_{j,\mathbf{k}'}^{\mathbb{T}})\varphi_{j,\mathbf{k},\mathbf{l}}^0 d\mathbf{x}, \qquad [\mathbf{f}_j]_{(\mathbf{k},\mathbf{l})} = \int_{\Omega_j} f\varphi_{j,\mathbf{k},\mathbf{l}}^0 d\mathbf{x},$$

$$[\mathbf{B}_j]_{k,\mathbf{k}'} = \int_0^1 (\varphi_{j,\mathbf{k}'}^{\mathbb{T}} \circ \boldsymbol{\gamma})\varphi_k^\Gamma d\phi, \qquad [\mathbf{g}_j]_k = \int_0^1 (g \circ \boldsymbol{\gamma})\varphi_k^\Gamma d\phi.$$

where $\boldsymbol{\gamma}$ denotes a suitable parameterization to Γ according to (1.8).

In order to tackle the different norms we need some suitable preconditioners. To compute the $H^{3/2}(\Gamma)$-norm of a function $g_j \in V_j^\Gamma$ we simply have to scale the

coefficients of $\sin(k\phi)$, and of $\cos(k\phi)$, by $k^{3/2}$. Thus, we shall introduce the diagonal matrix

$$[\mathbf{D}_j]_{k,l} = |k|^{3/2}\delta_{k,l}.$$

For preconditioning of the operator M we could use (as is done in [22]) a suitable wavelet transform, see e.g. [3]. Instead, we use the Bramble-Pasciak-Xu (BPX) multilevel preconditioner [2] associated with the discretization of $I - \mathrm{div}(\mathbf{A}\nabla)$. We indicate its application by the matrix $\mathbf{T}_j$.

We are now in the position to present the discrete least-squares problem: solve

$$(2.4) \qquad \left\| \begin{bmatrix} \mathbf{A}_j \\ \mathbf{D}_j\mathbf{B}_j \end{bmatrix} \mathbf{T}_j\mathbf{v}_j - \begin{bmatrix} \mathbf{f}_j \\ \mathbf{D}_j\mathbf{g}_j \end{bmatrix} \right\| \to \min$$

and take $\mathbf{u}_j^+ = \mathbf{T}_j\mathbf{v}_j$.

We use the iterative least-squares solver LSQR [26] to solve the discrete least-squares problem (2.4) iteratively within a nested iteration. Moreover, it is not necessary to assemble the matrix $\mathbf{B}_j$ since matrix-vector products $\mathbf{B}_j\mathbf{x}$ and $\mathbf{B}_j^T\mathbf{x}$ can be efficiently evaluated by using the (inverse) fast Fourier transform.

2.3. **Error estimates.** The energy space of the least-squares formulation (2.1) is the Sobolev space $H^2(\mathbb{T})$. Therefore, since we use ansatz functions that are exact of order m, the best possible convergence rate is limited by h_j^{2m-4}, achieved in the $H^{4-m}(\mathbb{T})$-norm if $u^+ \in H^m(\mathbb{T})$.

Theorem 2.1. *Assume that there exists an $n \in [0, m-2]$ such that*

$$(2.5) \qquad \|u - u_j\|_{H^{2-n}(\Omega)} \lesssim h_j^{2n}\|u\|_{H^{2+n}(\Omega)}$$

provided that $u \in H^{2+n}(\Omega)$. Then, if Γ is sufficiently smooth, the approximate shape functional and gradient

$$\widetilde{J}(\Omega) = \int_\Omega fu_j d\mathbf{x}, \qquad \widetilde{\nabla J}(\Omega)[\mathbf{U}] = \int_\Gamma \langle \mathbf{U}, \mathbf{n}\rangle\langle \mathbf{A}\nabla u_j, \nabla u_j\rangle d\sigma,$$

satisfy the error estimates

$$|J(\Omega) - \widetilde{J}(\Omega)| = \mathcal{O}(h_j^{2n}), \qquad |\nabla J(\Omega)[\mathbf{U}] - \widetilde{\nabla J}(\Omega)[\mathbf{U}]| = \mathcal{O}(h_j^{\min\{2n,n+1\}}).$$

Proof. The approximation error of the shape functional is estimated according to

$$\begin{aligned}
|J(\Omega) - \widetilde{J}(\Omega)| &= \left| \int_\Omega fu d\mathbf{x} - \int_\Omega fu_j d\mathbf{x} \right| \\
&\lesssim \|f\|_{H^{n-2}(\Omega)}\|u - u_j\|_{H^{2-n}(\Omega)} \\
&\lesssim h_j^{2n}\|f\|_{H^{n-2}(\Omega)}\|u\|_{H^{n-2}(\Omega)}.
\end{aligned}$$

In case of the shape gradient we derive the assertion by

$$|\nabla J(\Omega)[\mathbf{U}] - \widetilde{\nabla J}(\Omega)[\mathbf{U}]| = \left|\int_\Gamma \langle \mathbf{U}, \mathbf{n}\rangle \big\{\langle \mathbf{A}\nabla u, \nabla u\rangle - \langle \mathbf{A}\nabla u_j, \nabla u_j\rangle\big\} d\sigma\right|$$

$$\leq \left|\int_\Gamma \langle \mathbf{U}, \mathbf{n}\rangle \langle \mathbf{A}\nabla(u - u_j), \nabla(u - u_j)\rangle d\sigma\right| + 2\left|\int_\Gamma \langle \mathbf{A}\nabla u\langle \mathbf{U}, \mathbf{n}\rangle, \nabla(u - u_j)\rangle d\sigma\right|$$

$$\lesssim \|\langle \mathbf{U}, \mathbf{n}\rangle\|_{L^\infty(\Gamma)}\|u - u_j\|^2_{H^1(\Gamma)} + 2\|\nabla u\langle \mathbf{U}, \mathbf{n}\rangle\|_{H^{1/2}(\Gamma)}\|u - u_j\|_{H^{1/2}(\Gamma)}.$$

Using (2.5) together with the inverse inequality yields for the first term

$$\|\langle \mathbf{U}, \mathbf{n}\rangle\|_{L^\infty(\Gamma)}\|u - u_j\|^2_{H^1(\Gamma)} \lesssim h_j^{2n}\|\langle \mathbf{U}, \mathbf{n}\rangle\|_{L^\infty(\Gamma)}\|u\|^2_{H^{2+n}(\Gamma)}.$$

Invoking additionally the trace theorem the second term can be likewise estimated by

$$\|\nabla u\langle \mathbf{U}, \mathbf{n}\rangle\|_{H^{1/2}(\Gamma)}\|u - u_j\|_{H^{1/2}(\Gamma)} \lesssim \|\nabla u\langle \mathbf{U}, \mathbf{n}\rangle\|_{H^{1/2}(\Gamma)}\|u - u_j\|_{H^1(\Omega)}$$

$$\lesssim h_j^{\min\{2n, n+1\}}\|\langle \mathbf{U}, \mathbf{n}\rangle\|_{C^1(\Gamma)}\|u\|^2_{H^{2+n}(\Omega)}.$$

$\square$

2.4. **Computing domain integrals.** At least in order to evaluate the Dirichlet energy (1.1) we have to approximate domain integrals

$$(2.6) \qquad\qquad I(\Omega) := \int_\Omega f(\mathbf{x})d\mathbf{x}$$

for $f \in C(\overline{\Omega})$. This will be done as follows.

We compute the points of intersection of the boundary curve Γ and the underlying grid $\bigcup_{\mathbf{k}\in\mathbb{Z}} \partial Q_{j,\mathbf{k}}$. Then, we replace the boundary curve Γ by the piecewise linear curve $\widetilde{\Gamma}$ which connects these points by straight lines. The enclosed polygonal domain will be denoted by $\widetilde{\Omega}$.

We will next construct a suitable triangulation of $\widetilde{\Omega}$. We subdivide all elements $Q_{j,\mathbf{k}}$ that intersect the boundary $\widetilde{\Gamma}$ into suitable triangles to triangulate $Q_{j,\mathbf{k}} \cap \widetilde{\Omega}$. In the remaining part of $\widetilde{\Omega}$ we subdivide the elements $Q_{j,\mathbf{k}}$ into two triangles. Finally, we apply appropriate quadrature formulae for triangles. Figure 1 exemplifies a triangulation produced by our algorithm.

Theorem 2.2. *Assume that $\Omega \in C^2$ and $f \in C^2(\mathbb{D})$. Then, the above quadrature algorithm computes the integral $I(\Omega)$ from (2.6) with accuracy $\mathcal{O}(h_j^2)$ provided that the element quadrature formulae are exact for linear polynomials.*

Proof. The triangulation consists of $\mathcal{O}(h_j^{-2})$ elements of volume $\mathcal{O}(h_j^2)$. Consequently, since the element quadrature formulae are exact of order two, we get an error of quadrature $\mathcal{O}(h_j^4)$ per element. Thus, denoting the result of the composite quadrature
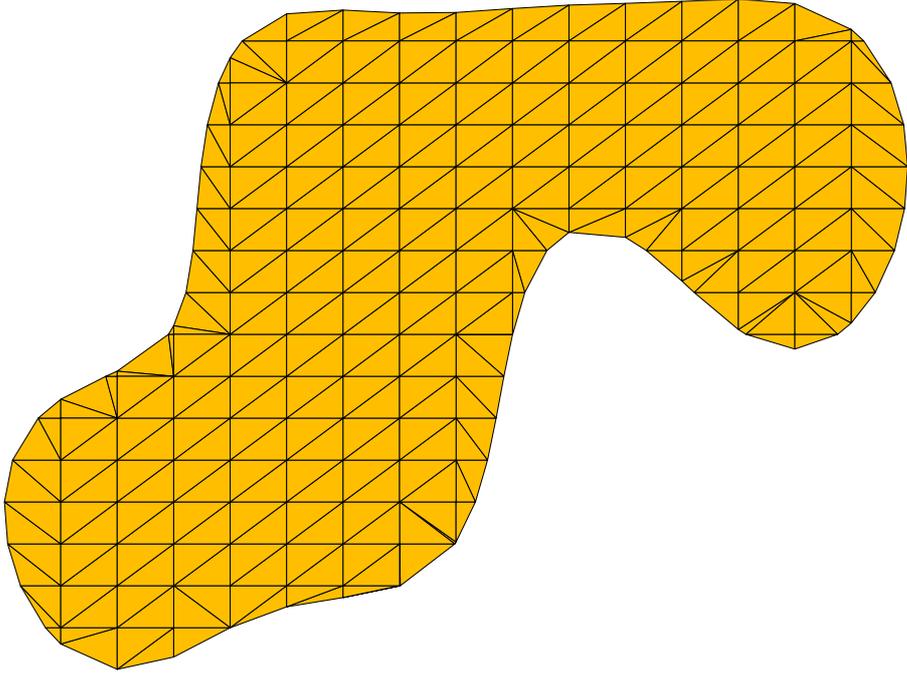
FIGURE 1. Triangulation of the domain.

formula by $Q(\widetilde{\Omega})$, we conclude

$$(2.7) \qquad\qquad |I(\widetilde{\Omega}) - Q(\widetilde{\Omega})| = \mathcal{O}(h_j^2).$$

We shall next estimate the error induced by the domain approximation. Since $\widetilde{\Gamma}$ is a piecewise linear approximation of step width $\sim h_j$ to the boundary curve Γ, the area $V(Q_{j,\mathbf{k}} \cap \Omega)$ of each square $Q_{j,\mathbf{k}}$ for which $Q_{j,\mathbf{k}} \cap \widetilde{\Gamma} \neq \emptyset$ is approximated of order

$$|V(Q_{j,\mathbf{k}} \cap \widetilde{\Omega}) - V(Q_{j,\mathbf{k}} \cap \Omega)| = \mathcal{O}(h_j^3).$$

Taking into account that there are at most $\mathcal{O}(h_j^{-1})$ squares that intersect the boundary curve, we conclude

$$(2.8) \qquad\qquad |I(\Omega) - I(\widetilde{\Omega})| = \mathcal{O}(h_j^2).$$

Combining both estimates yields the assertion due to

$$|I(\Omega) - Q(\Omega)| \leq |I(\Omega) - I(\widetilde{\Omega})| + |I(\widetilde{\Omega}) - Q(\widetilde{\Omega})|.$$

$\square$

Remark 2.3. *In three dimensions one introduces a triangulation of the free surface and henceforth a tretrahedral mesh of the domain. As one readily verifies the same error estimate holds while the complexity of the algorithm is $\mathcal{O}(h_j^{-3})$ instead $\mathcal{O}(h_j^{-2})$.*
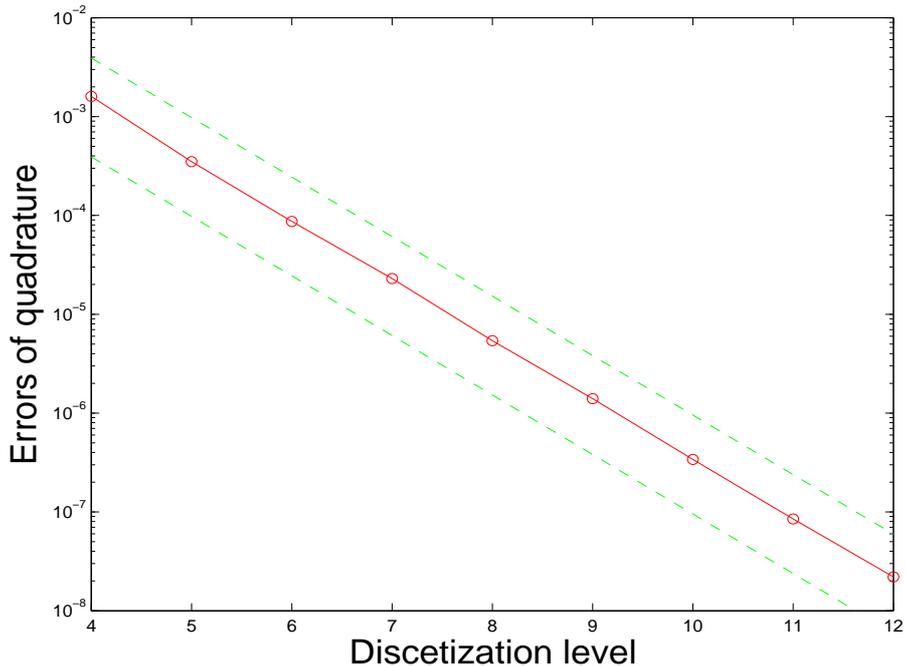
FIGURE 2. Errors of quadrature.

3. NUMERICAL EXPERIMENTS

3.1. **Domain quadrature.** We shall first demonstrate the domain quadrature algorithm, introduced in Subsection 2.4. The error estimate derived in Theorem 2.2 is sharp as the following example shows.

For different discretization levels j we approximate the volume of the domain that underlies the Figure 1. By virtue of the Gauss theorem, we can compare these values with the result of the following boundary integral

$$V(\Omega) = \frac{1}{2} \int_\Omega \text{div } \mathbf{x} \, d\mathbf{x} = \frac{1}{2} \int_\Gamma \langle \mathbf{x}, \mathbf{n} \rangle d\sigma,$$

computed with high accuracy. Notice that, even though $f \equiv 1$ in (2.6), this example validates the essential part of the error since it is related to the approximation error of the domain of integration (2.8). Whereas, the quadrature error on the perturbed domain depends only on the chosen quadrature rules and the smoothness of the integrand.

We plotted the errors of quadrature in semi-logarithmical scale in Figure 2. One observes in fact the predicted quadratic order of convergence in h_j, as indicated by dahed lines.

3.2. **Solving the state equation.** We next investigate the asymptotic behaviour of our fictitious domain solver. We use lowest order ansatz functions, that are quadratic smoothest splines ($m = 3$), and discontinuous piecewise bilinear test functions ($n = 2$).

To measure the rates of convergence of the smoothness preserving fictitious domain method we will focus on a boundary value problem where the solution is known analytically. To that end, we consider the following boundary value problem

$$-\operatorname{div}(\mathbf{A}\nabla u) = \cos(x)\big(4 + \sin^2(y)\big) - 6y\big(2 + \sin(x)\big) \text{ in } \Omega,$$
$$u = \cos(x) + y^3 \qquad\qquad\qquad \text{on } \Gamma,$$

where

$$\mathbf{A}(x,y) = \begin{bmatrix} 4 - \sin^2(y) & -1 \\ -1 & 2 + \sin(x) \end{bmatrix}.$$

We choose the same domain Ω as underlying in Figure 1. One readily verifies that the solution is given by the function $u = \cos(x) + y^3$.

j	$\|u - u_j\|_{L^2(\Omega)}$	$\|\nabla(u - u_j)\|_{L^2(\Omega)}$	cpu-time
4	3.1e-5	1.5e-3	0.3 sec.
5	4.6e-6 (6.7)	3.9e-4 (3.9)	1 sec.
6	8.5e-7 (5.4)	9.8e-5 (4.0)	6 sec.
7	1.1e-7 (7.8)	2.4e-5 (4.0)	30 sec.
8	1.6e-8 (6.6)	6.1e-6 (4.0)	128 sec.
9	3.8e-9 (4.4)	1.5e-6 (4.0)	10 min.
10	8.5e-10 (4.5)	3.8e-7 (4.0)	44 min

TABLE 1. Errors of approximation and over-all computing times.

We compute the numerical solution u_j for different discretization levels j by the smoothness preserving fictitious domain method proposed in the previous section. Since $m = 3$ we expect in $H^1(\Omega)$ an at most quadratic rate of convergence. In Table 1 we tabulate the absolute errors with respect to the L^2-norm and H^1-seminorm on Ω, respectively. The bracketed values indicate the ratio of the previous error and the present error. It is about 4 which implies quadratic orders of convergence. We illustrated the different error curves also in Figure 3. As indicated by the dashed lines one observes in fact quadratic rates of convergence for both norms. According to Theorem 2.1 we can therefore deduce that both, the shape functional and the shape gradient, will be approximated with quadratic orders of convergence.

The last column of Table 1 refers to the over-all computing times to produce the approximate solution u_j. The present implementation is still on experimental level,
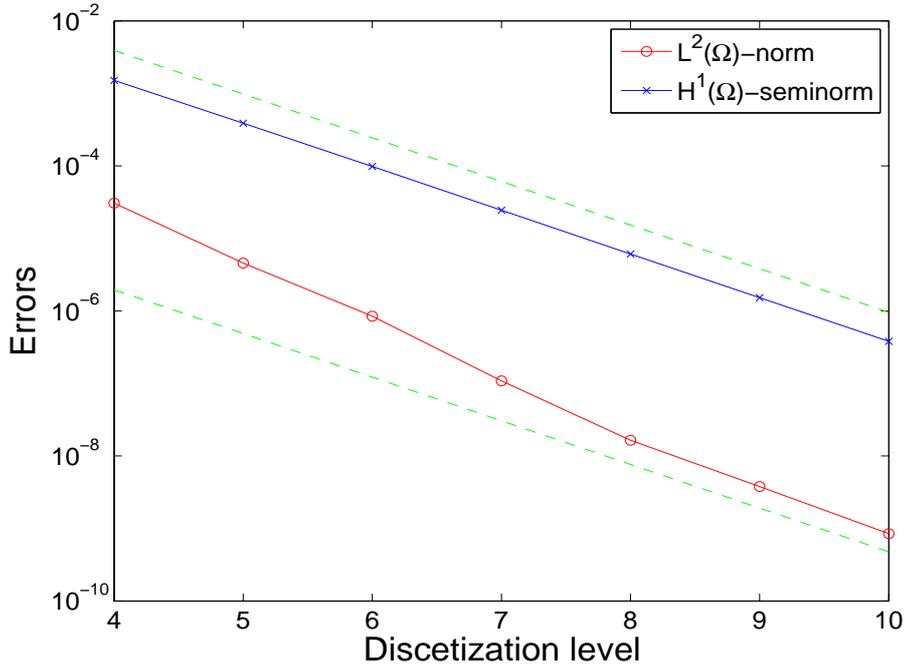
FIGURE 3. Rates of convergence.

being a mixture of MATLAB and C-Codes. Nevertheless, the method is feasible and highly accurate.

3.3. **Application to shape optimization problems.** We shall finally solve a shape optimization problem. We choose the diffusion matrix

$$\mathbf{A}(x,y) = \begin{bmatrix} 4 + 2.75\sin(10x) & -1 \\ -1 & 2 + \sin(3x) \end{bmatrix}$$

and the inhomogenity

$$f(x,y) = 2(1 - 3x^2)(1 - 3y^2)$$

as the data of the state equation (1.2) Moreover, we consider the volume constraint $V(\Omega) \overset{!}{=} V_0 := 0.2$.

The numerical setting is as follows. To approximate the boundary curve we choose $N = 16$ which yields 66 shape design parameters (cf. Subsection 1.4). Moreover, we perform 5 inner and 20 outer iterations of the augmented Lagrangian algorithm (cf. Subsection 1.3), where $\alpha := 100$ does a good job (see (1.6)). The regularization parameter is chosen as $\beta^{(n)} = 2^{-n}/100$ where n denotes the number of the outer iteration. The discretization level of the fictitious domain method is set to $j := 7$.

The domain computed by our algorithm is shown in Figure 3.3. The algorithm consumes about 1 hour cpu-time to derive this solution. To be on safe ground we
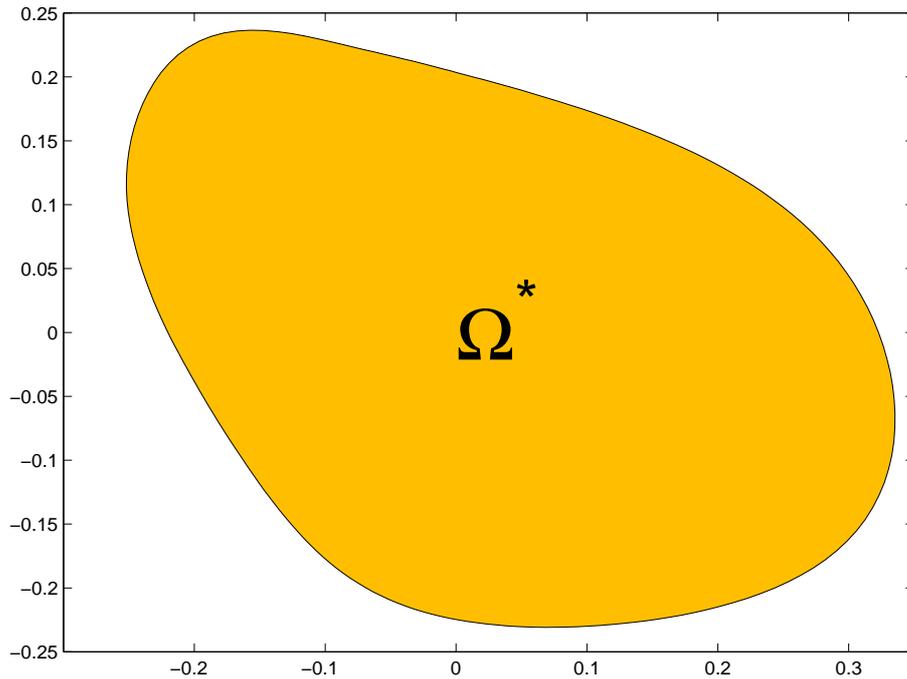
FIGURE 4. The maximizing domain.

validated the result by comparing it with the solution of a shape optimization algorithm based on starlike domains and finite elements (on starlike domains one can define the triangulation via parametrization). The maximizing domains produced by the different algorithms coincide.

4. CONCLUDING REMARKS

In the present paper we applied the novel smoothness preserving fictitious domain method from [22, 23] to a shape optimization problem. We derived discretization techniques which are applicable to two and three dimensional problems. Numerical results demonstrated that the new fictitious domain method is a quite promising meshless pde-solver as required for the development of fast and robust algorithms in shape optimization.

REFERENCES

[1] I. Babuška. The finite element method with Lagrangian multipliers. *Numer. Math.*, 20:179–192 (1973).

[2] J. Bramble, J.E. Pasciak, and J. Xu. Parallel multilevel preconditioners. *Math. Comp.*, 55:1–22, (1990).

[3] W. Dahmen. Wavelet and multiscale methods for operator equations. *Acta Numerica*, 6:55–228 (1997).

[4] M. Delfour and J.-P. Zolesio. *Shapes and Geometries.* SIAM, Philadelphia, 2001.

[5] J.E. Dennis and R.B. Schnabel. *Numerical Methods for Nonlinear Equations and Unconstrained Optimization Techniques.* Prentice-Hall, Englewood Cliffs, 1983.

[6] K. Eppler. Optimal shape design for elliptic equations via BIE-methods. *J. of Applied Mathematics and Computer Science*, 10:487–516, 2000.

[7] K. Eppler. Second derivatives and sufficient optimality conditions for shape functionals. *Control and Cybernetics*, 29:485–512, 2000.

[8] K. Eppler and H. Harbrecht. 2nd Order Shape Optimization using Wavelet BEM. *Optim. Methods Softw.*, 21:135–153, 2006.

[9] K. Eppler and H. Harbrecht. Efficient treatment of stationary free boundary problems. *WIAS-Preprint 965*, WIAS Berlin, 2004. submitted to Appl. Numer. Math.

[10] K. Eppler and H. Harbrecht. Exterior Electromagnetic Shaping using Wavelet BEM. *Math. Meth. Appl. Sci.* 28:387–405 (2005).

[11] K. Eppler and H. Harbrecht. Fast wavelet BEM for 3d electromagnetic shaping. *Appl. Numer. Math.* 54:537–554 (2005).

[12] K. Eppler and H. Harbrecht. Coupling of FEM and BEM in Shape Optimization. *WIAS-Preprint 1029*, WIAS Berlin, 2005. to appear in Numer. Math.

[13] A.V. Fiacco and G.P. McCormick. *Nonlinear Programming: Sequential Unconstrained Minimization Techniques.* Wiley, New York, 1968.

[14] R. Fletcher. *Practical Methods for Optimization, volume 1,2.* Wiley, New York, 1980.

[15] J. Haslinger and P. Neitaanmäki. *Finite element approximation for optimal shape, material and topology design, 2nd edition.* Wiley, Chichester, 1996.

[16] J. Haslinger und R.A.E. Mäkinen. Introduction to shape optimization. Theory, approximation and computation. Advances in Design and Control, vol. 7, SIAM Philadelphia, 2003.

[17] R. Glowinski, T.W. Pan, R.O. Wells, Jr., and X. Zhou. Wavelet and finite element solutions for the Neumann problem using fictitious domains. *J. Comp. Phys.*, 126:40–51 (1996).

[18] R. Glowinski, T.W. Pan, and J. Periaux. A fictitious domain method for Dirichlet problem and applications. *Comput. Methods Appl. Mech. Eng.*, 111(3–4):283–303 (1994).

[19] Ch. Grossmann and J. Terno. *Numerik der Optimierung.* Teubner, Stuttgart, 1993.

[20] H. Harbrecht and T. Hohage. Fast Methods for Three-Dimensional Inverse Obstacle Scattering. *Preprint 35/2005*, Institut für Numerische und Angewandte Mathematik, Georg-August-Universität Göttingen, 2005. submitted to J. Integral Equations Appl.

[21] K. Kunisch and G. Peichl. Shape optimization for mixed boundary value problems on an embedding domain method. *Dyn. Contin. Discrete Impulsive Syst.*, 4:439–478 (1998).

[22] M.S. Mommer. A Smoothness Preserving Fictitious Domain Method for Elliptic Boundary Value Problems. *IMA J. Numer. Anal.*, doi:10.1093/imanum/dri045 (2005)

[23] M.S. Mommer. Towards a Fictitious Domain Method with Optimally Smooth Solutions. PhD thesis, RWTH-Aachen, published online by the RWTH-Aachen (2005).

[24] F. Murat and J. Simon. Étude de problémes d'optimal design. in *Optimization Techniques, Modeling and Optimization in the Service of Man*, edited by J. Céa, Lect. Notes Comput. Sci. 41, Springer-Verlag, Berlin, 54–62 (1976).

[25] P. Neitaanmäki und D. Tiba. An embedding of domain approach in free boundary problems and optimal design. SIAM J. Control Optim., 33:1587–1602 (1995).

[26] C.C. Paige and M.A. Saunders. LSQR: An algorithm for sparse linear equations and sparse least squares. *ACM Trans. Math. Soft.*, 8:43–71 (1982).

[27] O. Pironneau. *Optimal shape design for elliptic systems*. Springer, New York, 1983.

[28] J. Simon. Differentiation with respect to the domain in boundary value problems. *Numer. Funct. Anal. Optimization* 2:649–687, 1980.

[29] T. Slawig. Domain optimization for the stationary Stokes and Navier–Stokes equations by an embedding domain technique. PhD Thesis, TU Berlin, 1998.

[30] T. Slawig. A formula for the derivative with respect to domain variations in Navier–Stokes flow based on an embedding domain method. *SIAM J. Control Optim.*, 42:495–512 (2003).

[31] J. Sokolowski and J.-P. Zolesio. *Introduction to Shape Optimization*. Springer, Berlin, 1992.

Karsten Eppler, Weierstrass Institut für Angewandte Analysis und Stochastik, Mohrenstr. 39, 10117 Berlin, Germany.

E-mail address: `eppler@math.wias-berlin.de`

Helmut Harbrecht, Institut für Informatik und Praktische Mathematik, Christian–Albrechts–Universität zu Kiel, Olshausenstr. 40, 24098 Kiel, Germany.

E-mail address: `hh@numerik.uni-kiel.de`

Mario Mommer, Department of Mathematics, Utrecht University, Budapestlaan 6, 3508 TA Utrecht, The Netherlands.

E-mail address: `mommer@math.uu.nl`